New physics effects in $\Lambda_b \to \Lambda \ell^+ \ell^-$ decay with lepton polarizations

T. M. Aliev[a] *, A. Özpineci[b] †, M. Savcı[a] ‡

a Physics Department, Middle East Technical University, 06531 Ankara, Turkey

b The Abdus Salam International Center for Theoretical Physics, I-34100, Trieste, Italy

Abstract

We study lepton polarization asymmetries in the $\Lambda_b \to \Lambda \ell^+ \ell^-$ decay using the most general model independent effective Hamiltonian. The dependence of the lepton polarizations and their combinations on the new Wilson coefficients are studied in detail. It is observed that there is a region for the new Wilson coefficients for which the branching ratio coincides with the standard model prediction, while lepton polarizations show considerable departure from standard model.

PACS numbers: 12.60.–i, 13.30.–a, 14.20.Mr

*e-mail: taliev@metu.edu.tr

†e-mail: ozpineci@ictp.trieste.it

‡e-mail: savci@metu.edu.tr

1 Introduction

Flavor–changing neutral current (FCNC) $b \to s(d)\ell^+\ell^-$ decays provide important tests for the gauge structure of the standard model (SM) at one–loop level. Moreover, $b \to s(d)\ell^+\ell^-$ decay is also very sensitive to the new physics beyond SM. New physics effects manifest themselves in rare decays in two different ways, either through new combinations to the new Wilson coefficients or through the new operator structure in the effective Hamiltonian which is absent in the SM. One of the efficient ways in establishing new physics beyond the SM is the measurement of the lepton polarization [1]–[8].

In this paper we investigate the possibility of searching for new physics in the heavy baryon decays $\Lambda_b \to \Lambda\ell^+\ell^-$ using the most general model independent form of effective Hamiltonian.

The main problem for the description of exclusive decays is to evaluate the form factors, i.e., matrix elements of the effective Hamiltonian between initial and final hadron states. It is well known that for describing baryonic $\Lambda_b \to \Lambda\ell^+\ell^-$ decay quite some number of form factors are needed (see for example [9]). However, when heavy quark effective theory (HQET) is applied only two independent form factors appear [10].

It should be mentioned here that the exclusive decay $\Lambda_b \to \Lambda\ell^+\ell^-$ decay is studied in the SM, the two Higgs doublet model and using the general form of the effective Hamiltonian, in [9], [11] and [12], respectively.

The sensitivity of the lepton polarizations to the new Wilson coefficients in the $B \to K^*\ell^+\ell^-$ decay is investigated in [13] using the general form of the Hamiltonian. It is shown in this work that the lepton polarizations are very sensitive to the scalar and tensor interactions. In this connection it is natural to ask to which new Wilson coefficients the lepton polarizations are strongly sensitive, in the "heavy baryon $\to$ light baryon $\ell^+\ell^-$" decays. In the present work we try to answer this question.

The paper is organized as follows. In section 2, using the most general form of the four–Fermi interaction, the general expressions for the longitudinal, transversal and normal polarizations of leptons are derived. In section 3 we investigate the sensitivity of these polarizations, as well as combined polarizations of lepton and antilepton to the new Wilson coefficients.

2 Lepton polarizations

In order to calculate lepton polarization in $\Lambda_b \to \Lambda\ell^+\ell^-$ decay, we start with the effective Hamiltonian for the $b \to \ell^+\ell^-$ transition. This effective Hamiltonian can be written in terms of twelve model independent four–Fermi interactions [8],

$$\begin{aligned}
\mathcal{M} = \frac{G\alpha}{4\sqrt{2}\pi} V_{tb}V_{ts}^* \Bigg\{ & C_{SL}\bar{s} i\sigma_{\mu\nu}\frac{q^\nu}{q^2} L b \bar{\ell}\gamma_\mu \ell + C_{BR}\bar{s} i\sigma_{\mu\nu}\frac{q^\nu}{q^2} b\bar{\ell}\gamma_\mu\ell + C_{LL}^{tot}\bar{s}_L\gamma^\mu b_L \bar{\ell}_L\gamma_\mu\ell_L \\
&+ C_{LR}^{tot}\bar{s}_L\gamma^\mu b_L\bar{\ell}_R\gamma_\mu\ell_R + C_{RL}\bar{s}_R\gamma^\mu b_R\bar{\ell}_L\gamma_\mu\ell_L + C_{RR}\bar{s}_R\gamma^\mu b_R\bar{\ell}_R\gamma_\mu\ell_R \\
&+ C_{LRLR}\bar{s}_L b_R\bar{\ell}_L\ell_R + C_{RLLR}\bar{s}_R b_L\bar{\ell}_L\ell_R + C_{LRRL}\bar{s}_L b_R\bar{\ell}_R\ell_L + C_{RLRL}\bar{s}_R b_L\bar{\ell}_R\ell_L \\
&+ C_T\bar{s}\sigma^{\mu\nu}b\bar{\ell}\sigma_{\mu\nu}\ell + iC_{TE}\epsilon^{\mu\nu\alpha\beta}\bar{s}\sigma_{\mu\nu}s\sigma_{\alpha\beta}\ell \Bigg\} , \qquad (1)
\end{aligned}$$

where $L = (1-\gamma_5)/2$ and $R = (1+\gamma_5)/2$ are the chiral operators. The coefficients of the first two terms, C_{SL} and C_{BR} are the nonlocal Fermi interactions, which correspond to $-2m_s C_7^{eff}$ and $-2m_b C_7^{eff}$ in the SM, respectively. The next four terms with coefficients C_{LL}^{tot}, C_{LR}^{tot}, C_{RL} and C_{RR} in Eq. (1) describe vector type interactions. Two of these coefficients C_{LL}^{tot} and C_{LR}^{tot} contain SM results in the form $C_9^{eff} - C_{10}$ and $C_9^{eff} - C_{10}$, respectively. For this reason we can write

$$\begin{aligned} C_{LL}^{tot} &= C_9^{eff} - C_{10} + C_{LL} \ , \\ C_{LR}^{tot} &= C_9^{eff} + C_{10} + C_{LL} \ , \end{aligned} \tag{2}$$

where C_{LL} and C_{LR} describe the contributions of new physics. The next four terms in Eq. (1) with coefficients C_{LRLR}, C_{RLLR}, C_{LRRL} and C_{RLRL} represent the scalar type interactions. The remaining last two terms leaded by the coefficients C_T and C_{TE} are the tensor type interactions.

The amplitude of the exclusive $\Lambda_b \to \Lambda \ell^+ \ell^-$ decay can be obtained by sandwiching $\mathcal{H}_{eff}$ for the $b \to s \ell^+ \ell^-$ transition between initial and final baryon states, i.e., $\langle \Lambda \left| \mathcal{H}_{eff} \right| \lambda_b \rangle$. It follows from Eq. (1) that in order to calculate the $\Lambda_b \to \Lambda \ell^+ \ell^-$ decay amplitude the following matrix elements are needed

$$\begin{aligned} &\langle \Lambda \left| \bar{s} \gamma_\mu (1 \mp \gamma_5) b \right| \Lambda_b \rangle \ , \\ &\langle \Lambda \left| \bar{s} \sigma_{\mu\nu} (1 \mp \gamma_5) b \right| \Lambda_b \rangle \ , \\ &\langle \Lambda \left| \bar{s} (1 \mp \gamma_5) b \right| \Lambda_b \rangle \ . \end{aligned}$$

Explicit forms of these matrix elements in terms of the form factors are presented in [12] (see also [9]). The matrix element of the $\Lambda_b \to \Lambda \ell^+ \ell^-$ can be written as

$$\begin{aligned} \mathcal{M} = \frac{G\alpha}{4\sqrt{2}\pi} V_{tb} V_{ts}^* \Bigg\{ & \bar{\ell} \gamma^\mu \ell \, \bar{u}_\Lambda \Big[A_1 \gamma_\mu (1+\gamma_5) + B_1 \gamma_\mu (1-\gamma_5) \\ & + i\sigma_{\mu\nu} q^\nu [A_2 (1+\gamma_5) + B_2 (1-\gamma_5)] + q_\mu [A_3 (1+\gamma_5) + B_3 (1-\gamma_5)] \Big] u_{\Lambda_b} \\ & + \bar{\ell} \gamma^\mu \gamma_5 \ell \, \bar{u}_\Lambda \Big[D_1 \gamma_\mu (1+\gamma_5) + E_1 \gamma_\mu (1-\gamma_5) + i\sigma_{\mu\nu} q^\nu [D_2 (1+\gamma_5) + E_2 (1-\gamma_5)] \\ & + q_\mu [D_3 (1+\gamma_5) + E_3 (1-\gamma_5)] \Big] u_{\Lambda_b} + \bar{\ell} \ell \, \bar{u}_\Lambda (N_1 + H_1 \gamma_5) u_{\Lambda_b} + \bar{\ell} \gamma_5 \ell \, \bar{u}_\Lambda (N_2 + H_2 \gamma_5) u_{\Lambda_b} \\ & + 4 C_T \bar{\ell} \sigma^{\mu\nu} \ell \, \bar{u}_\Lambda \Big[f_T \sigma_{\mu\nu} - i f_T^V (q_\nu \gamma_\mu - q_\mu \gamma_\nu) - i f_T^S (P_\mu q_\nu - P_\nu q_\mu) \Big] u_{\Lambda_b} \\ & + 4 C_{TE} \epsilon^{\mu\nu\alpha\beta} \bar{\ell} \sigma_{\alpha\beta} \ell \, i \bar{u}_\Lambda \Big[f_T \sigma_{\mu\nu} - i f_T^V (q_\nu \gamma_\mu - q_\mu \gamma_\nu) - i f_T^S (P_\mu q_\nu - P_\nu q_\mu) \Big] u_{\Lambda_b} \Bigg\} \ , \end{aligned} \tag{3}$$

where $P = p_{\Lambda_b} + p_\Lambda$. Explicit expressions of the functions A_i, B_i, D_i, E_i, H_j and N_j ($i = 1,2,3$ and $j = 1,2$) are given in [12].

From the expressions of the above-mentioned matrix elements we observe that $\Lambda_b \to \Lambda \ell^+ \ell^-$ decay is described in terms of many form factors. As has already been noted, when HQET is applied the number of independent form factors reduces to two (F_1 and F_2) irrelevant with the Dirac structure of the corresponding operators and it is obtained in [10] that

$$\langle \Lambda(p_\Lambda) \left| \bar{s} \Gamma b \right| \Lambda(p_{\Lambda_b}) \rangle = \bar{u}_\Lambda \Big[F_1(q^2) + \not{v} F_2(q^2) \Big] \Gamma u_{\Lambda_b} \ , \tag{4}$$

where Γ is an arbitrary Dirac structure, $v^\mu = p^\mu_{\Lambda_b}/m_{\Lambda_b}$ is the four–velocity of Λ_b, and $q = p_{\Lambda_b} - p_\Lambda$ is the momentum transfer. Comparing the general form of the form factors with (5), one can easily obtain the following relations among them (see also [9])

$$
\begin{aligned}
g_1 &= f_1 = f_2^T = g_2^T = F_1 + \sqrt{r} F_2 \ , \\
g_2 &= f_2 = g_3 = f_3 = g_T^V = f_T^V = \frac{F_2}{m_{\Lambda_b}} \ , \\
g_T^S &= f_T^S = 0 \ , \\
g_1^T &= f_1^T = \frac{F_2}{m_{\Lambda_b}} q^2 \ , \\
g_3^T &= \frac{F_2}{m_{\Lambda_b}} \left(m_{\Lambda_b} + m_\Lambda\right) \ , \\
f_3^T &= -\frac{F_2}{m_{\Lambda_b}} \left(m_{\Lambda_b} - m_\Lambda\right) \ ,
\end{aligned}
\tag{5}
$$

where $r = m^2_\Lambda / m^2_{\Lambda_b}$.

Having obtained the matrix element for the $\Lambda_b \to \Lambda \ell^+ \ell^-$ decay, our next aim is the calculation of lepton polarizations with the help of this matrix element. To achieve this goal we write the ℓ^- spin four–vector in terms of a unit vector $\vec{\xi}_\mp$ along the $\ell^\mp$ spin in its rest frame as

$$
s^\mp_\mu = \left(\frac{\vec{p}^{\,\mp} \cdot \vec{\xi}^{\,\mp}}{m_\ell}, \vec{\xi}^{\,\mp} + \frac{\vec{p}^{\,\mp} (\vec{p}^{\,\mp} \cdot \vec{\xi}^{\,\mp})}{E_\ell + m_\ell} \right) \ , \tag{6}
$$

and choose the unit vectors along the longitudinal, normal and transversal components of the ℓ^- polarization to be

$$
\vec{e}_L^{\,\mp} = \frac{\vec{p}^{\,\mp}}{|\vec{p}^{\,-}|} \ , \quad \vec{e}_N^{\,\mp} = \frac{\vec{p}_\Lambda \times \vec{p}^{\,\mp}}{|\vec{p}_\Lambda \times \vec{p}^{\,-}|} \ , \quad \vec{e}_T^{\,\mp} = \vec{e}_N^{\,\mp} \times \vec{e}_L^{\,\mp} \ , \tag{7}
$$

respectively, where $\vec{p}^{\,\mp}$ and $\vec{p}_\Lambda$ are the three momenta of $\ell^\mp$ and Λ, in the center of mass frame of the $\ell^+\ell^-$ system. Obviously, $\vec{p}^{\,+} = -\vec{p}^{\,-}$ in this reference frame.

The differential decay rate of the $\Lambda_b \to \Lambda \ell^+ \ell^-$ decay for any spin direction $\vec{\xi}^{\,\mp}$ along $\ell^\mp$ can be written as

$$
\frac{d\Gamma(\vec{\xi}^{\,\mp})}{ds} = \frac{1}{2} \left(\frac{d\Gamma}{ds} \right)_0 \left[1 + \left(P_L^\mp \vec{e}_L^{\,\mp} + P_N^\mp \vec{e}_N^{\,\mp} + P_T^\mp \vec{e}_T^{\,\mp} \right) \cdot \vec{\xi}^{\,\mp} \right] \ , \tag{8}
$$

where $(d\Gamma/ds)_0$ corresponds to the unpolarized differential decay rate, $s = q^2/m^2_{\Lambda_b}$ and $P_L^\mp$, $P_N^\mp$ and $P_T^\mp$ represent the longitudinal, normal and transversal polarizations of $\ell^\mp$, respectively. The unpolarized decay width in Eq. (8) can be written as

$$
\left(\frac{d\Gamma}{s} \right)_0 = \frac{G^2 \alpha^2}{8192 \pi^5} \left| V_{tb} V_{ts}^* \right|^2 \lambda^{1/2}(1, r, s) v \Big[\mathcal{T}_0(s) + \frac{1}{3} \mathcal{T}_2(s) \Big] \ , \tag{9}
$$

where $\lambda(1, r, s) = 1 + r^2 + s^2 - 2r - 2s - 2rs$ is the triangle function and $v = \sqrt{1 - 4m^2_\ell / q^2}$ is the lepton velocity. The explicit expressions for $\mathcal{T}_0$ and $\mathcal{T}_2$ can be found in [12].

The polarizations P_L, P_N and P_T are defined as:

$$P_i^{(\mp)}(q^2) = \frac{\frac{d\Gamma}{ds}(\vec{\xi}^{\,\mp} = \vec{e}_i^{\,\mp}) - \frac{d\Gamma}{ds}(\vec{\xi}^{\,\mp} = -\vec{e}_i^{\,\mp})}{\frac{d\Gamma}{ds}(\vec{\xi}^{\,\mp} = \vec{e}_i^{\,\mp}) + \frac{d\Gamma}{ds}(\vec{\xi}^{\,\mp} = -\vec{e}_i^{\,\mp})} ~,$$

where $i = L, N, T$. P_L and P_T are P–odd, T–even, while P_N is P–even, T–odd and CP–odd. The explicit forms of the lepton polarizations P_L, P_T and P_N can be found in Appendix–A.

It follows from Eq. (A.1) that the difference between $P_L^-(P_N^-)$ and $P_L^+(P_N^+)$ can be attributed to the existence of the scalar and tensor interactions. Again in the same way, in massless lepton case, the difference between P_T^- and P_T^+ results from scalar and vector interactions. For this reason these above–mentioned polarizations are sensitive to the chiral structure of the electroweak interactions and can serve as a useful tool in search of new physics beyond the SM.

Combined analysis of the lepton and antilepton polarizations can give additional information about the existence of new physics, since in the SM $P_L^- + P_L^+ = 0$, $P_N^- + P_N^+ = 0$ and $P_T^- - P_T^+ \simeq 0$ (in $m_\ell \to 0$ limit). Therefore if nonzero values for the above mentioned combined asymmetries are measured in the experiments, it can be considered as an unambiguous indication of the existence of new physics.

3 Numerical analysis

In this section we will study the dependence of the lepton polarizations, as well as combined lepton polarization to the new Wilson coefficients. The main input parameters in the calculations are the form factors. Since the literature lacks exact calculations for the form factors of the $\Lambda_b \to \Lambda$ transition, we will use the results from QCD sum rules approach in combination with HQET [10, 14], which reduces the number of quite many form factors into two. The s dependence of these form factors can be represented in the following way

$$F(q^2) = \frac{F(0)}{1 - a_F s + b_F s^2} ~,$$

where parameters $F_i(0)$, a and b are listed in table 1.

	$F(0)$	a_F	b_F
F_1	0.462	-0.0182	-0.000176
F_2	-0.077	-0.0685	0.00146

Table 1: Transition form factors for $\Lambda_b \to \Lambda \ell^+ \ell^-$ decay in the QCD sum rules method.

We use the next–to–leading order logarithmic approximation for the resulting values of the Wilson coefficients C_9^{eff}, C_7 and C_{10} in the SM [15, 16] at the renormalization point $\mu = m_b$. It should be noted that, in addition to short distance short distance contribution, C_9^{eff} receives also long distance contributions from the real $\bar{c}c$ resonant states of the J/ψ

family. In the present work we do not take into account the long distance effects. In order to perform quantitative analysis of the lepton polarizations the values of the new Wilson coefficients, which describe the new physics beyond the SM, are needed. In the foregoing numerical analysis we vary all new Wilson coefficients in the range $-|C_{10}| \leq C_X \leq |C_{10}|$. The experimental bounds on the branching ratio of the $B \to K^* \mu^+\mu^-$ and $B_s \to \mu^+\mu^-$ [17] suggest that this is the right order of magnitude range for the vector and scalar interaction coefficients. Furthermore we assume that all new Wilson coefficients are real.

Before performing numerical analysis, few words about lepton polarizations are in order. From explicit expressions of the lepton polarizations one can easily see that they depend on both s and the new Wilson coefficients. For this reason it may experimentally be problematic to study their dependence on these variables simultaneously. Therefore we will eliminate the dependence of the lepton polarization on one of the variables. We choose to eliminate the variable s by performing integration over s in the allowed kinematical region, so that lepton polarizations are averaged over. The averaged lepton polarizations are defined as

$$\langle P_i \rangle = \frac{\displaystyle\int_{4m_\ell^2/m_{\Lambda_b}^2}^{(1-\sqrt{r})^2} P_i \frac{d\mathcal{B}}{ds} ds}{\displaystyle\int_{4m_\ell^2/m_{\Lambda_b}^2}^{(1-\sqrt{r})^2} \frac{d\mathcal{B}}{ds} ds} \ . \tag{10}$$

The dependence of the averaged lepton polarizations $\left\langle P_L^- \right\rangle$, $\left\langle P_T^- \right\rangle$ and $\left\langle P_N^- \right\rangle$ on the new Wilson coefficients are shown in Figs (1)–(3). From these figures we obtain the following results.

- $\left\langle P_L^- \right\rangle$ is strongly dependent to the tensor interaction for both μ and τ channels. In the τ channel it is also sensitive to the scalar interaction with coefficient C_{LRRL}. More over it is observed that $\left\langle P_L^- \right\rangle$ is negative for all values of the new Wilson coefficients in the μ channel, while it is positive for $C_T \lesssim -1.7$ and $C_T \gtrsim 0.5$ for the τ case.

- $\left\langle P_T^- \right\rangle$ is strongly dependent to the scalar interaction C_{LRRL}, as well as to the tensor interaction for the μ channel. The τ channel is strongly dependent on the tensor interaction. From Fig. (2a) we see that $\left\langle P_T^- \right\rangle$ is negative (positive) for the μ channel when $C_{LRRL} \lesssim -1.5$ ($C_{LRRL} \gtrsim -1.5$), $C_T \gtrsim 0.75$ ($C_T \lesssim 0.75$) and $C_{TE} \lesssim -0.5$ ($C_{LRRL} \gtrsim -0.5$). For τ channel the situation is different and $\left\langle P_T^- \right\rangle$ is positive when $C_T \lesssim -2.6$ and $C_T \gtrsim 0.6$ and is negative for all other values of the new Wilson coefficients.

- It follows from Eq. (A.3) that the normal polarization is proportional to the imaginary parts of the combination of the products of the new Wilson coefficients. However, since in this work we assume that all new Wilson coefficients are real, the nonzero value of $\left\langle P_N^- \right\rangle$ is due to the imaginary part of the C_9^{eff} only. Moreover, since $\left\langle P_N^- \right\rangle$ is proportional to the lepton mass, it is maximum value is around 1% for the μ channel and therefore we do not present its dependence on the new Wilson coefficients. For the τ case $\left\langle P_N^- \right\rangle$ shows stronger dependence on C_{LL}, C_{LRRL}, as well as on C_T. It is interesting to note that $\left\langle P_N^- \right\rangle$ is positive when $C_T \lesssim -1.25,\ c_T \gtrsim 0.7$, while it is negative for all other cases.

Our numerical analysis for the combined lepton, antilepton polarizations leads to the following results.

- $\left\langle P_L^- + P_L^+ \right\rangle$ is strongly dependent only to the scalar type interactions and quite weakly on the remaining new Wilson coefficients. $\left\langle P_L^- + P_L^+ \right\rangle$ is positive (negative) when C_{RLRL}, C_{LRRL} are negative (positive) and C_{RLLR}, C_{LRLR} are positive (negative). The magnitude of $\left\langle P_L^- + P_L^+ \right\rangle$ for the μ channel varies between -0.15 and 0.15 depending on the variation of the scalar interaction.

  For τ case, $\left\langle P_L^- + P_L^+ \right\rangle$ exhibits strong dependence on the tensor interaction C_T and scalar interactions C_{LRLR} and C_{LRRL}. $\left\langle P_L^- + P_L^+ \right\rangle$ is positive (negative) when $C_T \lesssim 0$ ($C_T \gtrsim 0$) and the sign of the scalar interactions are negative (positive). The value of $\left\langle P_L^- + P_L^+ \right\rangle$ for this case varies between -0.35 and 0.4 depending on the variation of the corresponding tensor and scalar interactions. It should be noted that $\left\langle P_L^- + P_L^+ \right\rangle = 0$ in the SM.

- The situation for the combined $\left\langle P_T^- - P_T^+ \right\rangle$ polarization is as follows. For the μ channel, $\left\langle P_T^- - P_T^+ \right\rangle$ is strongly dependent on the tensor interactions C_T, C_{TE} and the scalar C_{LRLR}, C_{LRRL} coefficients when $C_{TE} \lesssim -0.5$, $C_T \gtrsim 0.9$, $C_{LRLR} \gtrsim 2$ and $C_{LRRL} \lesssim -2$, $\left\langle P_T^- - P_T^+ \right\rangle$ is negative and for all other cases it is positive. The magnitude of $\left\langle P_T^- - P_T^+ \right\rangle$ varies between the values $(-0.2 \div 0.45)$ depending on the variation of the scalar and tensor interaction coefficients.

  When we investigate the τ case, $\left\langle P_T^- - P_T^+ \right\rangle$ is observed to be strongly dependent on tensor interactions. $\left\langle P_T^- - P_T^+ \right\rangle$ is negative only for $C_{TE} \gtrsim 1.2$, otherwise it is positive. The magnitude of $\left\langle P_T^- - P_T^+ \right\rangle$ for the τ channel lies in the region $(-0.01 \div 0.98)$ depending on the variation of the tensor interaction coefficient.

- The final analysis we present is the combined $\left\langle P_N^- + P_N^+ \right\rangle$ polarization, which essentially shows dependence only on C_T and C_{TE}. Its value ranges between -0.015 and 0.035 depending on the variation of the tensor interactions.

From these analyzes we can conclude that the change in sign and magnitude of both $\left\langle P_i^- \right\rangle$ and $\left\langle P_i^- + (-) P_i^+ \right\rangle$ ($-$ sign is for the transversal polarization case) is an indication of the existence of new physics beyond the SM.

At the and of our analysis, we would like to discuss about the following problem. The branching ratio of the $\Lambda_b \to \Lambda \ell^- \ell^+$ decay depends also on the new Wilson coefficients. Moreover its experimental measurement is easier compared to the case with the lepton polarizations. One could ask then what advantage the measurement with lepton polarizations has, since similar information can be attained from the branching ratio measurement. Obviously, measurement of lepton polarizations are quite useful for establishing new physics if we can find the parameter space of the new Wilson coefficients in which the decay rate agrees with the SM while the lepton polarizations deviate considerably from the SM case. The intriguing question is whether there exist such a region for the new Wilson coefficients C_X. In order to answer this question we present in Figs. (4)–(8) the correlation between the branching ratio and the averaged and averaged–combined lepton polarizations for the $\Lambda_b \to \Lambda \ell^- \ell^+$ decay. In Fig. (4) we present the correlation in the $\left(\mathcal{B}, \left\langle P_L^- \right\rangle\right)$ plane by varying the coefficients of the scalar, vector and tensor type interactions. Depicted in Fig. (5) is the correlation in the $\left(\mathcal{B}, \left\langle P_L^- + P_L^+ \right\rangle\right)$ plane by varying the coefficients of the new scalar, vector and tensor type interactions. In these figures the value of the branching ratio is restricted to have the values in the region $2 \times 10^{-7} \leq \mathcal{B}(\Lambda_b \to \Lambda \tau^+ \tau^-) \leq 5 \times 10^{-7}$ which is quite close to the SM prediction.

We observe from these figures that, indeed there exist regions for the new Wilson coefficients for which $\left\langle P_L^- \right\rangle$ and $\left\langle P_L^- + P_L^+ \right\rangle$ show considerable departure from the SM prediction, while branching ratio coincide with the SM result.

Our numerical results show that the case for the transversal, normal and the combined polarizations $\left\langle P_T^- - P_T^+ \right\rangle$ and $\left\langle P_N^- + P_N^+ \right\rangle$, one can find similar regions of the new Wilson coefficients with branching ratios coinciding with the SM results while lepton polarizations differing considerably (see Figs. (7),(8)).

In conclusion, we present the most general analysis of the lepton polarizations in the exclusive $\Lambda_b \to \Lambda \ell^- \ell^+$ decay, using the general, model independent form of the effective Hamiltonian. The sensitivity of the longitudinal, transversal and normal polarizations of ℓ^-, as well as lepton–antilepton combined asymmetries on the new Wilson coefficients, are studied. We find out that there exist regions in the parameter space of the new Wilson coefficients, in which branching ratios coincide with the SM results while lepton polarizations differ considerably. A thorough study of the lepton polarizations in this region of the parameter space of the new Wilson coefficients can establish new physics beyond the SM.

Appendix A : **Lepton polarizations**

In this appendix we present the explicit form of the expressions for the longitudinal P_L, transversal P_T and normal P_N lepton polarizations. The $-(+)$ sign in these formulas corresponds to the particle (antiparticle), respectively.

$$
\begin{aligned}
P_L^{\mp} = & \frac{256}{3}\lambda m_\ell m_{\Lambda_b}^5 v(1+\sqrt{r}) \,\mathrm{Re}[(A_1+B_1)^* C_{TE} f_T^S \pm (D_1+E_1)^* C_T f_T^S] \\
& + 32 m_\ell m_{\Lambda_b}^3 v(1+\sqrt{r})[s-(1-\sqrt{r})^2] \,\mathrm{Re}[(D_1-E_1)^* H_1] \\
& - 32 m_\ell m_{\Lambda_b}^3 v(1-\sqrt{r})[s-(1+\sqrt{r})^2] \,\mathrm{Re}[(D_1+E_1)^* F_1] \\
& + \frac{512}{3}\lambda m_{\Lambda_b}^6 sv\Big(8\,\mathrm{Re}[C_T^* C_{TE}]\,\mathrm{Re}[f_T^* f_T^S] - m_\ell \,\mathrm{Re}[(A_2+B_2)^* C_{TE} f_T^S \pm (D_2+E_2)^* C_T f_T^S]\Big) \\
& - \frac{4096}{3}\lambda m_{\Lambda_b}^7 sv(1+\sqrt{r})\,\mathrm{Re}[C_T^* C_{TE}]\,\mathrm{Re}[f_T^{S*} f_T^V] \\
& \pm 64 m_{\Lambda_b}^4 sv\sqrt{r}\Big(2\,\mathrm{Re}[A_1^* E_1 + B_1^* D_1] - m_{\Lambda_b}(1-r+s)\,\mathrm{Re}[A_1^* D_2 + A_2^* D_1]\Big) \\
& \mp 64 m_{\Lambda_b}^5 \sqrt{r}(1-r+s) sv \,\mathrm{Re}[B_1^* E_2 + B_2^* E_1] \\
& - 512 m_{\Lambda_b}^5 sv(1+\sqrt{r})[s-(1-\sqrt{r})^2]\Big(8\,\mathrm{Re}[C_T^* C_{TE}]\,\mathrm{Re}[f_T^* f_T^V] \\
& - m_\ell \,\mathrm{Re}[(A_2+B_2)^* C_{TE} f_T^V \pm (D_2+E_2)^* C_T f_T^V]\Big) \\
& + \frac{2048}{3}\lambda m_{\Lambda_b}^8 sv[s-(1+\sqrt{r})^2]\left|f_T^S\right|^2 \,\mathrm{Re}[C_T^* C_{TE}] \\
& \pm 128 m_{\Lambda_b}^6 s^2 v\sqrt{r}\,\mathrm{Re}[A_2^* E_2 + B_2^* D_2] \\
& - 16 m_{\Lambda_b}^4 sv[s-(1+\sqrt{r})^2]\,\mathrm{Re}[F_1^* F_2 + 2m_\ell (D_3+E_3)^* F_1] \\
& - 16 m_{\Lambda_b}^4 sv[s-(1-\sqrt{r})^2]\,\mathrm{Re}[H_1^* H_2 + 2m_\ell (D_3-E_3)^* H_1] \\
& \pm 64 m_{\Lambda_b}^5 sv(1-r-s)\,\mathrm{Re}[A_1^* E_2 + A_2^* E_1 + B_1^* D_2 + B_2^* D_1] \\
& \mp \frac{64}{3} m_{\Lambda_b}^4 v[1+r^2+r(s-2)+s(1-2s)]\,\mathrm{Re}[A_1^* D_1 + B_1^* E_1] \\
& + \frac{512}{3} m_{\Lambda_b}^4 v[(1-r)^2+(1-6\sqrt{r}+r)s-2s^2]\Big(m_\ell \,\mathrm{Re}[(A_1+B_1)^* C_{TE} f_T^V \pm (D_1+E_1)^* C_T f_T^V] \\
& - 4 m_{\Lambda_b}^2 s\left|f_T^V\right|^2 \,\mathrm{Re}[C_T^* C_{TE}]\Big) \\
& - \frac{4096}{3} m_{\Lambda_b}^4 v[2(1-r)^2-(1+r)s-s^2]\left|f_T\right|^2 \,\mathrm{Re}[C_T^* C_{TE}] \\
& + \frac{256}{3} m_\ell m_{\Lambda_b}^4 v\Big\{(1+2\sqrt{r}+r-s)(2-4\sqrt{r}+2r+s)\,\mathrm{Re}[(B_2-A_2)^* C_T f_T] \\
& + 2(1-2\sqrt{r}+r-s)(2+4\sqrt{r}+2r+s)\,\mathrm{Re}[(B_2+A_2)^* C_{TE} f_T]\Big\} \\
& \pm \frac{512}{3} m_\ell m_{\Lambda_b}^4 v\Big\{(1-2\sqrt{r}+r-s)(2+4\sqrt{r}+2r+s)\,\mathrm{Re}[(D_2+E_2)^* C_T f_T] \\
& - 2(1+2\sqrt{r}+r-s)(2-4\sqrt{r}+2r+s)\,\mathrm{Re}[(D_2-E_2)^* C_{TE} f_T]\Big\} \\
& \mp \frac{64}{3} m_{\Lambda_b}^6 sv[2+r(2r-4-s)-s(1+s)]\,\mathrm{Re}[A_2^* D_2 + B_2^* E_2]
\end{aligned}
\qquad (A.1)
$$

$$
\begin{aligned}
&\mp 512 m_\ell m_{\Lambda_b}^3 v \Big\{ (1+\sqrt{r})(1-2\sqrt{r}+r-s)\,\mathrm{Re}[(D_1+E_1)^* C_T f_T] \\
&+ 2(1-\sqrt{r})(1+2\sqrt{r}+r-s)\,\mathrm{Re}[(D_1-E_1)^* C_{TE} f_T] \Big\} \\
&+ 256 m_\ell m_{\Lambda_b}^3 v \Big\{ (1-\sqrt{r})(1+2\sqrt{r}+r-s)\,\mathrm{Re}[(B_1-A_1)^* C_T f_T] \\
&- 2(1+\sqrt{r})(1-2\sqrt{r}+r-s)\,\mathrm{Re}[(B_1+A_1)^* C_{TE} f_T] \Big\}\ ,
\end{aligned}
$$

$$
\begin{aligned}
P_T^{\mp} =\ & -16\pi m_\ell m_{\Lambda_b}^3 \sqrt{s\lambda} \Big(|A_1|^2 - |B_1|^2 \Big) \\
&\mp 64\pi m_\ell m_{\Lambda_b}^3 \sqrt{s\lambda}\,\mathrm{Re}[(C_T F_2^* - 2C_{TE} H_2^*) f_T] \\
&\pm 128\pi m_\ell^2 m_{\Lambda_b}^3 \sqrt{s\lambda}\,\mathrm{Re}[2(D_3-E_3)^* C_{TE} f_T - (D_3+E_3)^* C_T f_T] \\
&+ 32\pi m_\ell m_{\Lambda_b}^4 \sqrt{s\lambda}\,\mathrm{Re}[A_1^* B_2 - A_2^* B_1] \\
&\mp 16\pi m_\ell m_{\Lambda_b}^4 \sqrt{s\lambda}\,\mathrm{Re}[A_1^* E_3 - A_2^* E_1 + B_1^* D_3 - B_2^* D_1] \\
&+ 4\pi m_{\Lambda_b}^4 \sqrt{s\lambda}(1-\sqrt{r}) \Big(\pm\,\mathrm{Re}[(A_1-B_1)^* H_2] + 512 m_\ell\,\mathrm{Re}[C_T C_{TE}^* f_T^* f_T^V] \Big) \\
&\mp 4\pi m_{\Lambda_b}^4 \sqrt{s\lambda}(1+\sqrt{r}) \Big(\mathrm{Re}[(A_1+B_1)^* F_2] - 16 m_\ell\,\mathrm{Re}[C_T F_2^* f_T^V] \\
&- 32 m_\ell^2\,\mathrm{Re}[(D_3+E_3)^* C_T f_T^V] \Big) \\
&+ 16\pi m_\ell m_{\Lambda_b}^5 \sqrt{s\lambda}(1-r) \Big(|A_2|^2 - |B_2|^2 \Big) \\
&+ 16\pi m_\ell m_{\Lambda_b}^4 \sqrt{rs\lambda}\,\mathrm{Re}[2A_1^* A_2 - 2B_1^* B_2 \mp A_1^* D_3 \mp A_2^* D_1 \mp B_1^* E_3 \mp B_2^* E_1] \\
&- 16\pi m_\ell m_{\Lambda_b}^3 \sqrt{\frac{\lambda}{s}}(1-r) \Big(\pm\,\mathrm{Re}[A_1^* D_1 + B_1^* E_1] + 128\,|f_T|^2\ \mathrm{Re}[C_T^* C_{TE}] \Big) \qquad \text{(A.2)} \\
&\pm 4\pi m_{\Lambda_b}^5 s\sqrt{s\lambda} \Big(\mathrm{Re}[(A_2+B_2)^* F_2 + (A_2-B_2)^* H_2] + 4m_\ell\,\mathrm{Re}[A_2^* D_3 + B_2^* E_3] \Big) \\
&\pm 128\pi m_\ell^2 m_{\Lambda_b}^4 \sqrt{\frac{\lambda}{s}}(1-\sqrt{r})[(1+\sqrt{r})^2 - s]\,\mathrm{Re}[(D_1+E_1)^* C_T f_T^S] \\
&\pm 64\pi m_\ell m_{\Lambda_b}^5 \sqrt{s\lambda}[(1+\sqrt{r})^2 - s] \Big(\mathrm{Re}[F_2^* C_T f_T^S] + 2m_\ell\,\mathrm{Re}[(D_3+E_3)^* C_T f_T^S] \Big) \\
&\mp 32\pi m_{\Lambda_b}^4 \sqrt{s\lambda}(1-2v^2) \Big\{ (1-\sqrt{r})\,\mathrm{Re}[(D_1+E_1)^* C_T f_T] \\
&+ 2(1+\sqrt{r})\,\mathrm{Re}[(D_1-E_1)^* C_{TE} f_T] \Big\} \\
&- 32\pi m_{\Lambda_b}^4 \sqrt{s\lambda}(2-v^2) \Big\{ (1+\sqrt{r})\,\mathrm{Re}[(A_1-B_1)^* C_T f_T] \\
&+ 2(1-\sqrt{r})\,\mathrm{Re}[(A_1+B_1)^* C_{TE} f_T] \Big\} \\
&+ 32\pi m_{\Lambda_b}^5 s\sqrt{s\lambda}(2-v^2) \Big(\mathrm{Re}[(A_1-B_1)^* C_T f_T^V] + m_{\Lambda_b}(1-\sqrt{r})\,\mathrm{Re}[(A_2-B_2)^* C_T f_T^V] \Big) \\
&- 32\pi m_{\Lambda_b}^5 \sqrt{s\lambda}(1-r)(2-v^2) \Big(\mathrm{Re}[(A_2-B_2)^* C_T f_T] - 2\,\mathrm{Re}[(A_2+B_2)^* C_{TE} f_T] \Big) \\
&+ 4\pi m_{\Lambda_b}^4 \sqrt{s\lambda} v^2 \Big\{ (1-\sqrt{r})\,\mathrm{Re}[(D_1-E_1)^* H_1] - (1+\sqrt{r})\,\mathrm{Re}[(D_1+E_1)^* F_1] \Big\} \\
&\mp 32\pi m_{\Lambda_b}^5 \sqrt{s\lambda}(1-r) v^2 \Big(\mathrm{Re}[(D_2+E_2)^* C_T f_T] - 2\,\mathrm{Re}[(D_2-E_2)^* C_{TE} f_T] \Big) \\
&+ 4\pi m_{\Lambda_b}^5 s\sqrt{s\lambda} v^2 \Big(\mathrm{Re}[(D_2+E_2)^* F_1] + \mathrm{Re}[(D_2-E_2)^* H_1] \Big) \\
&\mp 64\pi m_{\Lambda_b}^6 s\sqrt{s\lambda}(1-\sqrt{r}) v^2\,\mathrm{Re}[(D_2-E_2)^* C_{TE} f_T^V]
\end{aligned}
$$

$$\pm\, 64\pi m_{\Lambda_b}^3 \sqrt{\frac{\lambda}{s}} \Big\{ 2m_\ell^2 (1-r)\, \mathrm{Re}[(D_1+E_1)^* C_T f_T^V] - m_{\Lambda_b}^2 s^2 v^2\, \mathrm{Re}[(D_1-E_1)^* C_{TE} f_T^V] \Big\}\ ,$$

$$\begin{aligned}
P_N^{\mp} &= \pm 16\pi m_\ell m_{\Lambda_b}^3 v\sqrt{s\lambda} \Big(\mathrm{Im}[A_1^* D_1 - B_1^* E_1] + 4\,\mathrm{Im}[F_1^* C_T f_T] - 8\,\mathrm{Im}[H_1^* C_{TE} f_T] \Big) \\
&+ 16\pi m_\ell m_{\Lambda_b}^4 v\sqrt{s\lambda} \Big(\pm\, \mathrm{Im}[B_1^* D_2 - A_1^* E_2] + \mathrm{Im}[(\pm A_2 + D_2 + D_3)^* E_1] \\
&- \mathrm{Im}[(\pm B_2 - E_2 - E_3)^* D_1] \Big) \\
&+ 32\pi m_{\Lambda_b}^4 v\sqrt{s\lambda} \Big(\mathrm{Im}[B_1^* (C_T - 2C_{TE}) f_T] - \sqrt{r}\, \mathrm{Im}[B_1^* (C_T + 2C_{TE}) f_T] \Big) \\
&+ 4\pi m_{\Lambda_b}^4 v\sqrt{s\lambda} \Big\{ (1-\sqrt{r})\, \mathrm{Im}[\pm (A_1 - B_1)^* H_1 + (D_1 - E_1)^* H_2] \\
&- (1+\sqrt{r})\, \mathrm{Im}[\pm (A_1 + B_1)^* F_1 + (D_1 + E_1)^* F_2] \\
&- 128 m_\ell (1-\sqrt{r}) \left(4\, |C_{TE}|^2 - |C_T|^2 \right) \mathrm{Im}[f_T^* f_T^V] \Big\} \\
&\mp 64\pi m_\ell m_{\Lambda_b}^4 v\sqrt{s\lambda} (1+\sqrt{r})\, \mathrm{Im}[F_1^* C_T f_T^V] \\
&+ 32\pi m_{\Lambda_b}^4 v\sqrt{s\lambda} \Big(\mathrm{Im}[(A_1 \mp D_1 \pm \sqrt{r} E_1)^* (C_T + 2C_{TE}) f_T] \\
&- \mathrm{Im}[(\sqrt{r} A_1 \pm \sqrt{r} D_1 \mp E_1)^* (C_T - 2C_{TE}) f_T] \Big) \\
&- 32\pi m_{\Lambda_b}^5 v\sqrt{s\lambda} (1-r) \Big(\mathrm{Im}[(A_2 \pm D_2)^* (C_T - 2C_{TE}) f_T] + \mathrm{Im}[(B_2 \mp E_2)^* (C_T + 2C_{TE}) f_T] \Big) \\
&\mp 16\pi m_\ell m_{\Lambda_b}^4 v\sqrt{s\lambda} \Big(m_{\Lambda_b} (1-r)\, \mathrm{Im}[A_2^* D_2 - B_2^* E_2] + \sqrt{r}\, \mathrm{Im}[A_1^* D_2 + A_2^* D_1] \Big) \\
&+ 16\pi m_\ell m_{\Lambda_b}^4 v\sqrt{rs\lambda}\, \mathrm{Im}[D_1^* (D_2 - D_3) - E_2^* (\pm B_1 + E_1) - E_1^* (\pm B_2 + E_3)] \\
&+ 4\pi m_{\Lambda_b}^5 v s\sqrt{s\lambda}\, \mathrm{Im}[\pm (A_2 + B_2)^* F_1 + (D_2 + E_2)^* F_2] \\
&- 32\pi m_{\Lambda_b}^5 v s\sqrt{s\lambda}\, \mathrm{Im}[2(A_1 - B_1)^* C_{TE} f_T^V \mp (D_1 - E_1)^* C_T f_T^V] \\
&+ 4\pi m_{\Lambda_b}^5 v s\sqrt{s\lambda} \Big(\mathrm{Im}[\pm (A_2 - B_2)^* H_1 + (D_2 - E_2)^* H_2] + 4 m_\ell\, \mathrm{Im}[D_2^* D_3 + E_2^* E_3] \Big) \\
&- 32\pi m_{\Lambda_b}^6 v s\sqrt{s\lambda} (1-\sqrt{r}) \Big(\mathrm{Im}[2(A_2 - B_2)^* C_{TE} f_T^V \mp (D_2 - E_2)^* C_T f_T^V] \\
&\mp 64\pi m_\ell m_{\Lambda_b}^5 v\sqrt{s\lambda} [(1+\sqrt{r})^2 - s]\, \mathrm{Im}[F_1^* C_T f_T^S]\ ,
\end{aligned} \tag{A.3}$$

References

[1] J. L. Hewett, *Phys. Rev.* **D53** (1996) 4964.

[2] F. Krüger and L. M. Sehgal *Phys. Lett.* **B380** (1996) 199.

[3] Y. G. Kim, P. Ko, J. S. Lee, *Nucl. Phys.* **B544** (1999) 64.

[4] T. M. Aliev, M. Savcı, *Phys. Lett.* **B452** (1999) 318.

[5] T. M. Aliev, M. Savcı, *Phys. Lett.* **B452** (1999) 318;
T. M. Aliev, H. Koru, A. Özpineci, M. Savcı, *Phys. Lett.* **B410** (1997) 216.

[6] D. Guetta, E. Nardi, *Phys. Rev.* **D58** (1998) 012001.

[7] Chuan–Hung Chen and C. Q. Geng, *Phys. Lett.* **B516** (2001) 327.

[8] S. Fukae, C. S. Kim, T. Yoshikawa, *Phys. Rev.* **D61** (2000) 074015.

[9] Chuan–Hung Chen and C. Q. Geng, *Phys. Rev.* **D64** (2001) 074001.

[10] T. Mannel, W. Roberts and Z. Ryzak, *Nucl. Phys.* **B355** (1991) 38.

[11] T. M. Aliev, M. Savcı, *J. Phys.* **G26** (2000) 997.

[12] T. M. Aliev, A. Özpineci, M. Savcı, prep. hep–ph/0202120 (2002).

[13] T. M. Aliev, M. K. Çakmak, M. Savcı, *Nucl. Phys.* **B607** (2001) 305.

[14] C.–S. Huang, H.–G. Yan, *Phys. Rev.* **D59** (1999) 114022.

[15] C. Bobeth, M. Misiak, and J. Urban, *Nucl. Phys.* **B574** (2000) 291.

[16] H. H. Asatrian, H. M. Asatrian, C. Greub, and M. Walker, *Phys. Lett.* **B507** (2001) 162.

[17] CDF Collaboration, T. Affolder *at. al*, *Phys. Rev. Lett.* **83** (1999) 3378;
CLEO Collaboration, Yongsheng Gao, prep. hep–ex/0108005 (2001).

Figure captions

Fig. (1) The dependence of the averaged longitudinal lepton polarization $\left\langle P_L^- \right\rangle$ on the new Wilson coefficients for the $\Lambda_b \to \Lambda \ell^+ \ell^-,\ (\ell = \mu,\ \tau)$ decay.

Fig. (2) The same as in Fig. (1), but for the averaged transversal lepton polarization $\left\langle P_T^- \right\rangle$.

Fig. (3) The dependence of the averaged normal lepton polarization $\left\langle P_N^- \right\rangle$ on the new Wilson coefficients for the $\Lambda_b \to \Lambda \tau^+ \tau^-$ decay.

Fig. (4) Parametric plot of the correlation between the branching ratio $\mathcal{B}$ (in units of 10^{-7}) and the averaged longitudinal polarization $\left\langle P_L^- \right\rangle$ as a function of the new Wilson coefficients for the $\Lambda_b \to \Lambda \tau^+ \tau^-$ decay.

Fig. (5) The same as in Fig. (4), but for the combined averaged longitudinal lepton polarization $\left\langle P_L^- + P_L^+ \right\rangle$.

Fig. (6) The same as in Fig. (4), but for the averaged transversal lepton polarization $\left\langle P_T^- \right\rangle$.

Fig. (7) The same as in Fig. (4), but for the combined averaged transversal lepton polarization $\left\langle P_T^- - P_T^+ \right\rangle$.

Fig. (8) The same as in Fig. (4), but for the combined averaged normal lepton polarization $\left\langle P_N^- + P_N^+ \right\rangle$.

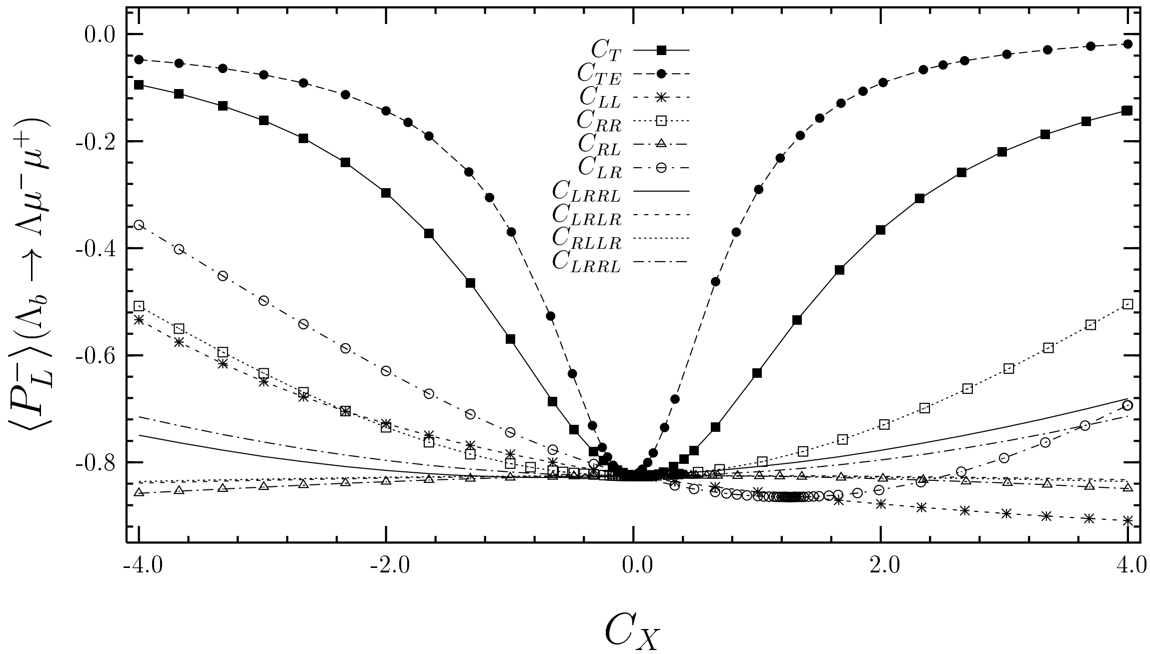

$\langle P_L^- \rangle(\Lambda_b \to \Lambda \mu^- \mu^+)$
C_X
C_T
C_{TE}
C_{LL}
C_{RR}
C_{RL}
C_{LR}
C_{LRRL}
C_{LRLR}
C_{RLLR}
C_{LRRL}
0.0
-0.2
-0.4
-0.6
-0.8
-4.0
-2.0
0.0
2.0
4.0

Fig. 1–a

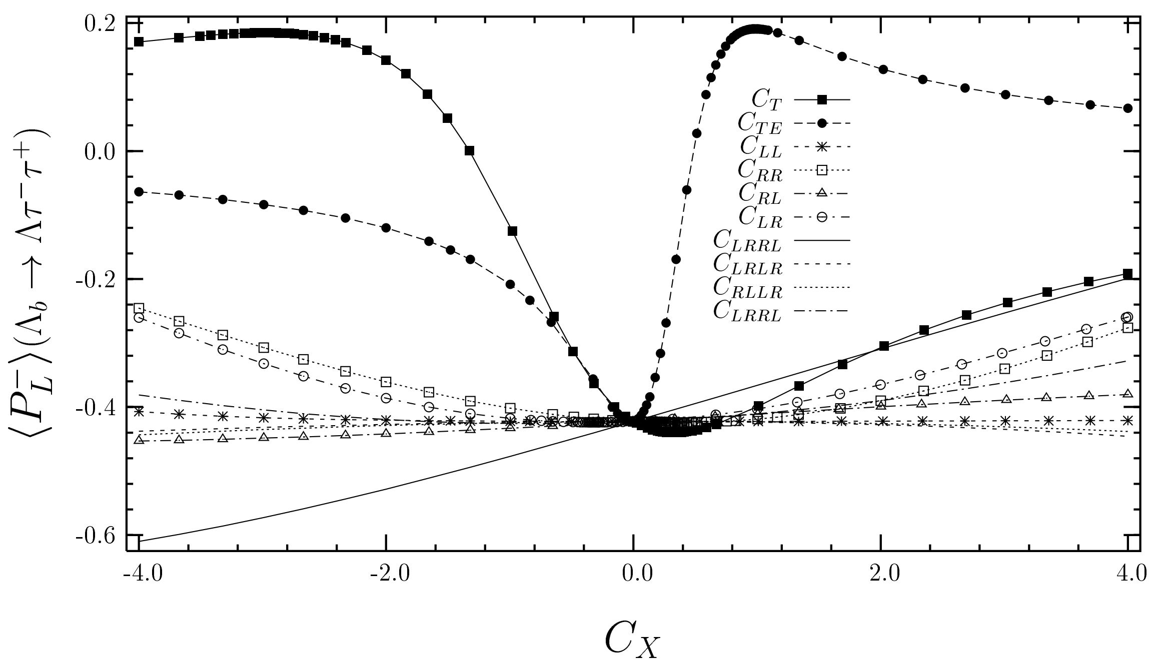

$\langle P_L^- \rangle(\Lambda_b \to \Lambda \tau^- \tau^+)$
C_X
C_T
C_{TE}
C_{LL}
C_{RR}
C_{RL}
C_{LR}
C_{LRRL}
C_{LRLR}
C_{RLLR}
C_{LRRL}
0.2
0.0
-0.2
-0.4
-0.6
-4.0
-2.0
0.0
2.0
4.0

Fig. 1–b

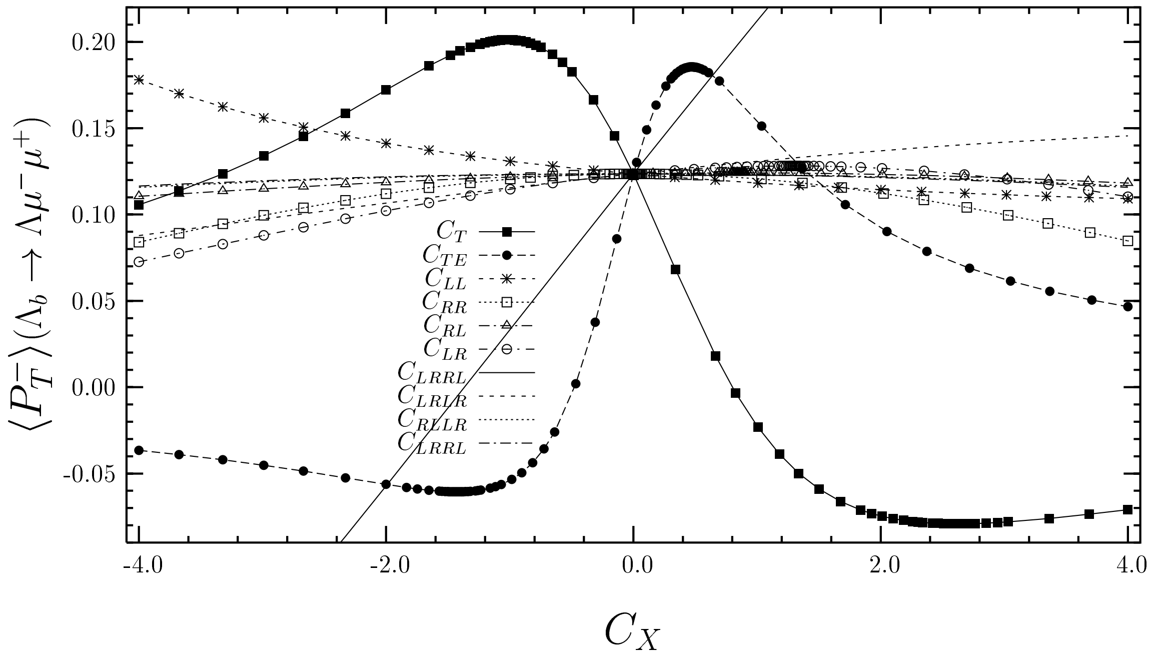

0.20
0.15
0.10
0.05
0.00
-0.05
-4.0
-2.0
0.0
2.0
4.0
$\langle P_T^- \rangle(\Lambda_b \to \Lambda \mu^- \mu^+)$
C_X
C_T
C_{TE}
C_{LL}
C_{RR}
C_{RL}
C_{LR}
C_{LRRL}
C_{LRLR}
C_{RLLR}
C_{LRRL}

Fig. 2–a

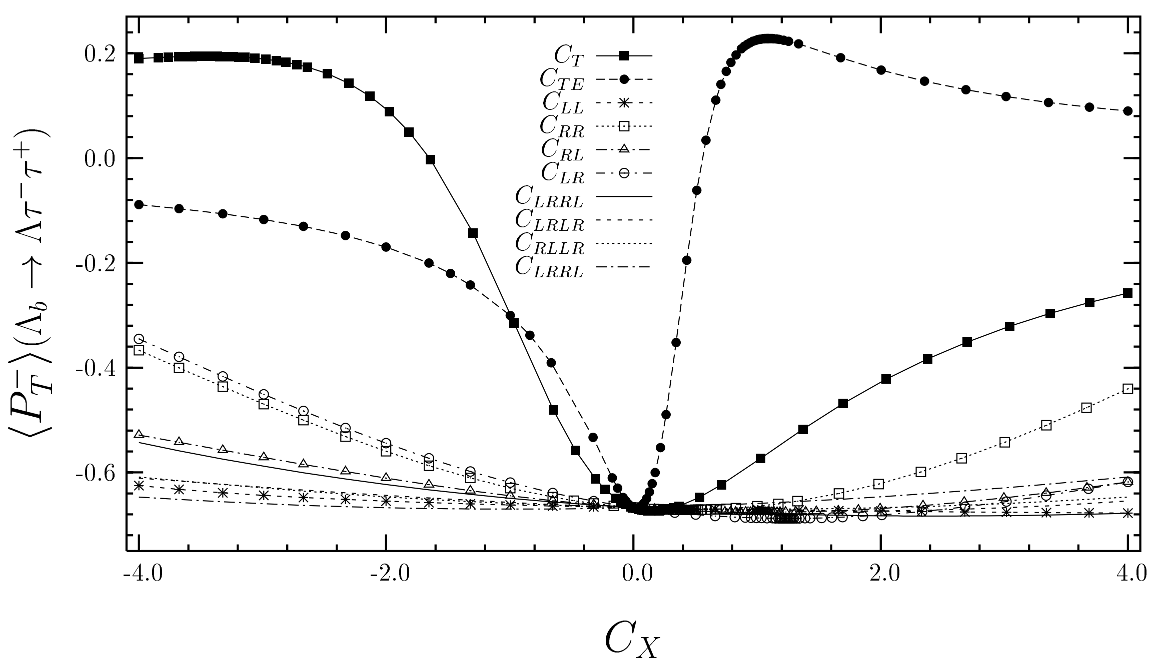

0.2
0.0
-0.2
-0.4
-0.6
-4.0
-2.0
0.0
2.0
4.0
$\langle P_T^- \rangle(\Lambda_b \to \Lambda \tau^- \tau^+)$
C_X
C_T
C_{TE}
C_{LL}
C_{RR}
C_{RL}
C_{LR}
C_{LRRL}
C_{LRLR}
C_{RLLR}
C_{LRRL}

Fig. 2–b

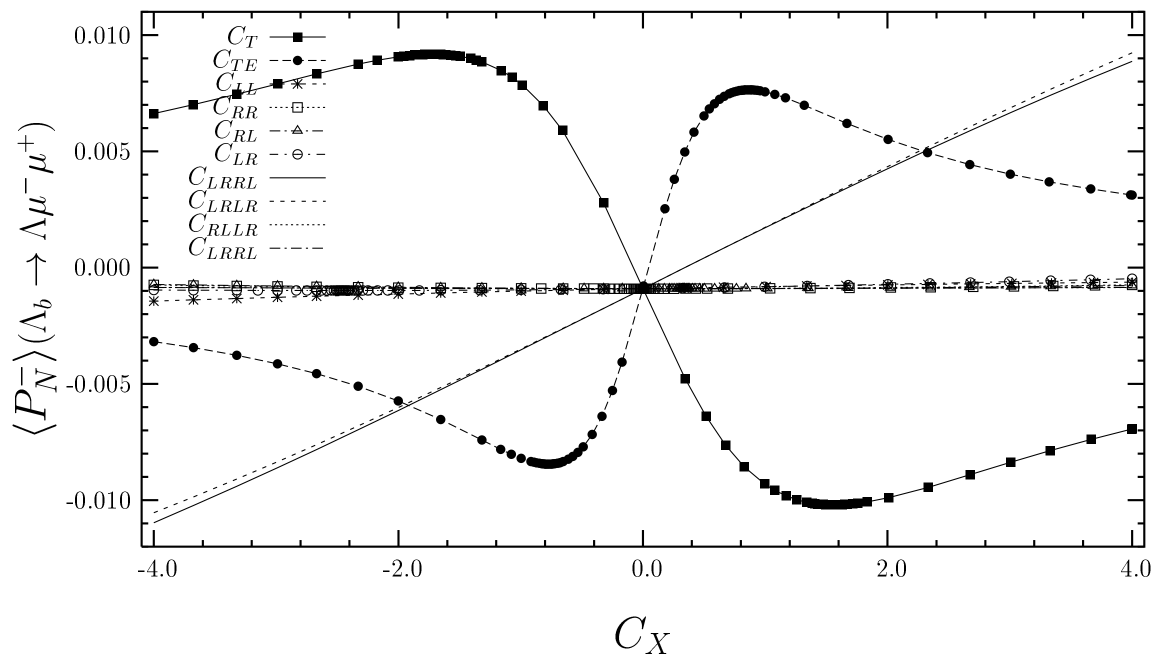
C_T
C_{TE}
C_{LL}
C_{RR}
C_{RL}
C_{LR}
C_{LRRL}
C_{LRLR}
C_{RLLR}
C_{LRRL}
$\langle P_N^- \rangle(\Lambda_b \to \Lambda \mu^- \mu^+)$
0.010
0.005
0.000
-0.005
-0.010
-4.0
-2.0
0.0
2.0
4.0
C_X

Fig. 3–a

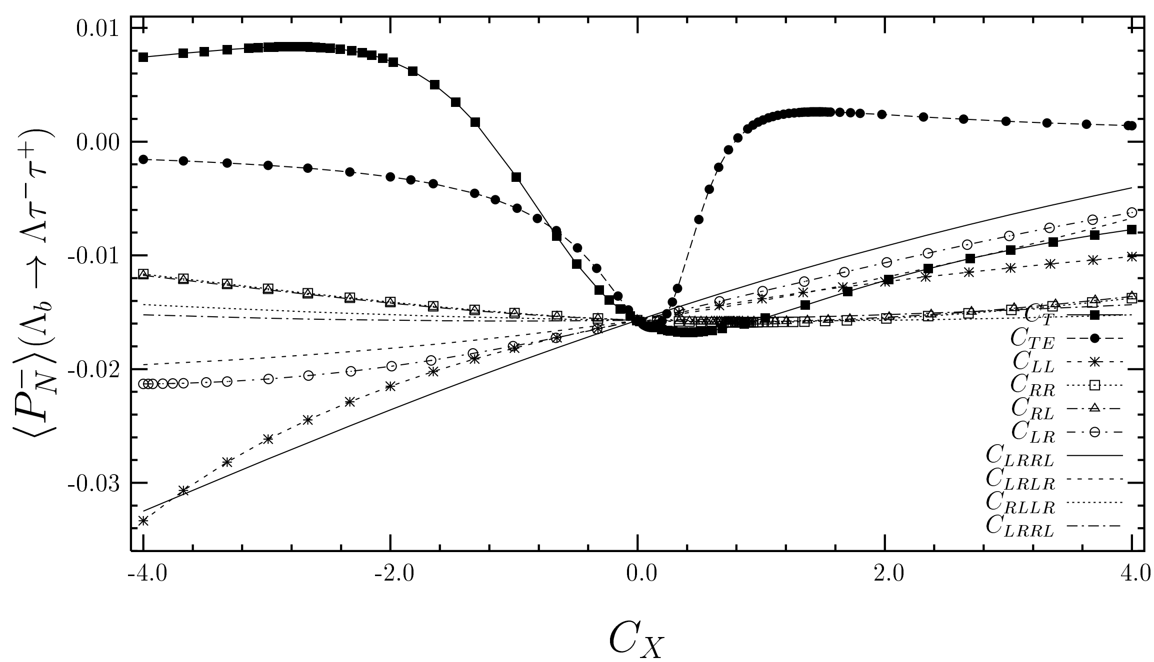
C_T
C_{TE}
C_{LL}
C_{RR}
C_{RL}
C_{LR}
C_{LRRL}
C_{LRLR}
C_{RLLR}
C_{LRRL}
$\langle P_N^- \rangle(\Lambda_b \to \Lambda \tau^- \tau^+)$
0.01
0.00
-0.01
-0.02
-0.03
-4.0
-2.0
0.0
2.0
4.0
C_X

Fig. 3–b

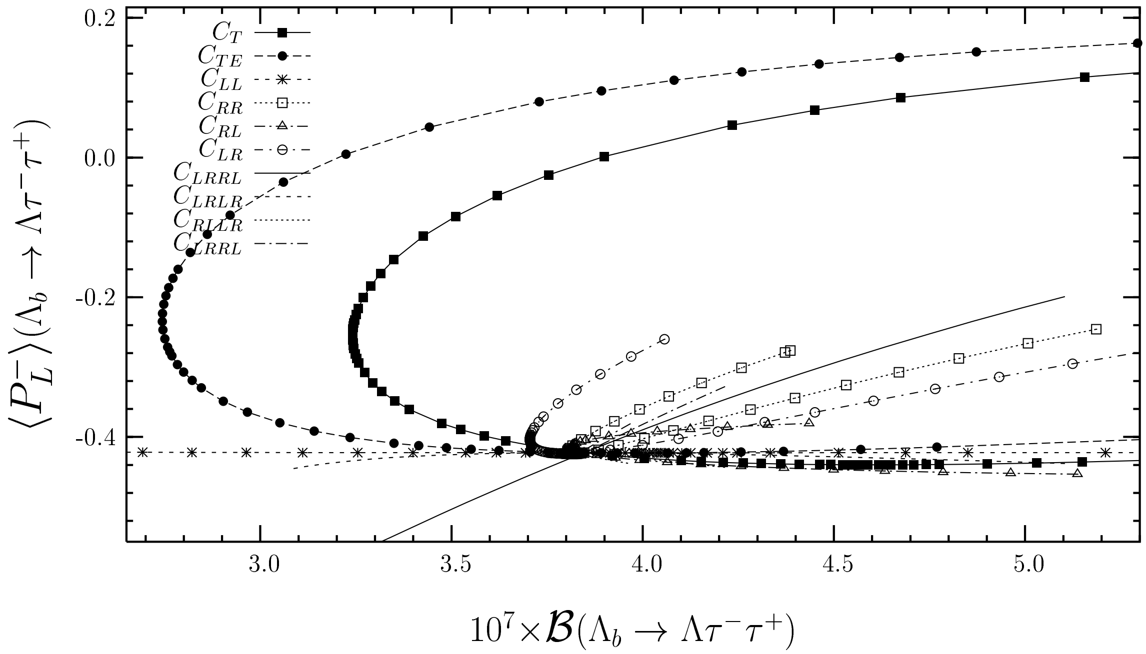

C_T
C_{TE}
C_{LL}
C_{RR}
C_{RL}
C_{LR}
C_{LRRL}
C_{LRLR}
C_{RLLR}
C_{LRRL}
0.2
0.0
-0.2
-0.4
3.0
3.5
4.0
4.5
5.0
$\langle P_L^- \rangle(\Lambda_b \to \Lambda \tau^- \tau^+)$
$10^7 \times \mathcal{B}(\Lambda_b \to \Lambda \tau^- \tau^+)$

Fig. 4

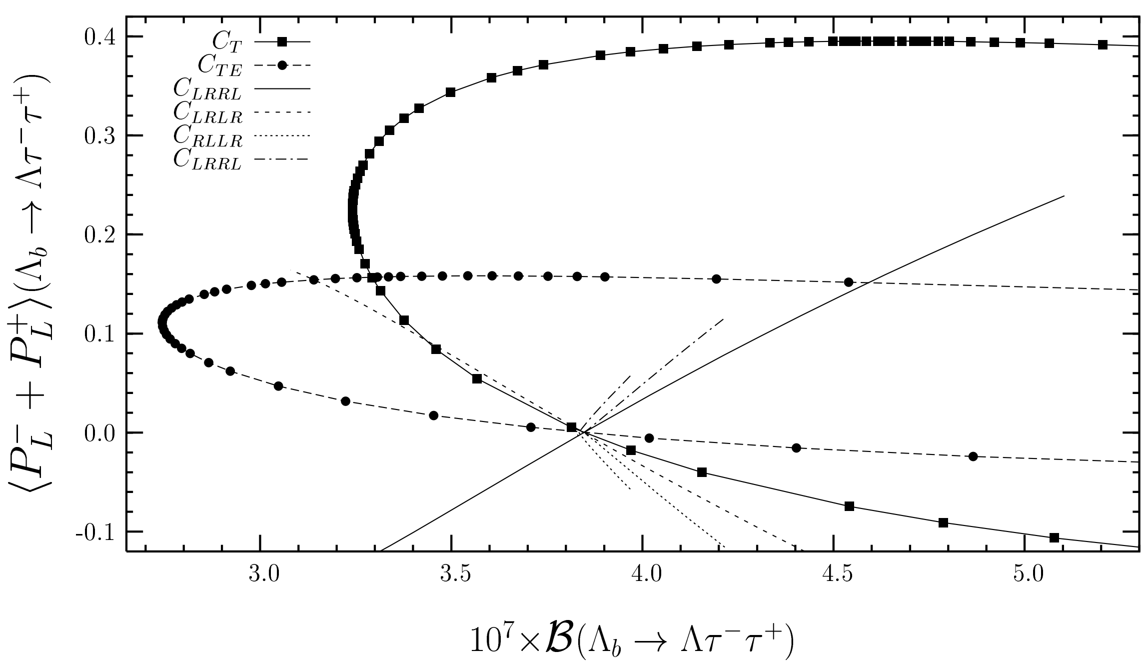

C_T
C_{TE}
C_{LRRL}
C_{LRLR}
C_{RLLR}
C_{LRRL}
0.4
0.3
0.2
0.1
0.0
-0.1
3.0
3.5
4.0
4.5
5.0
$\langle P_L^- + P_L^+ \rangle(\Lambda_b \to \Lambda \tau^- \tau^+)$
$10^7 \times \mathcal{B}(\Lambda_b \to \Lambda \tau^- \tau^+)$

Fig. 5

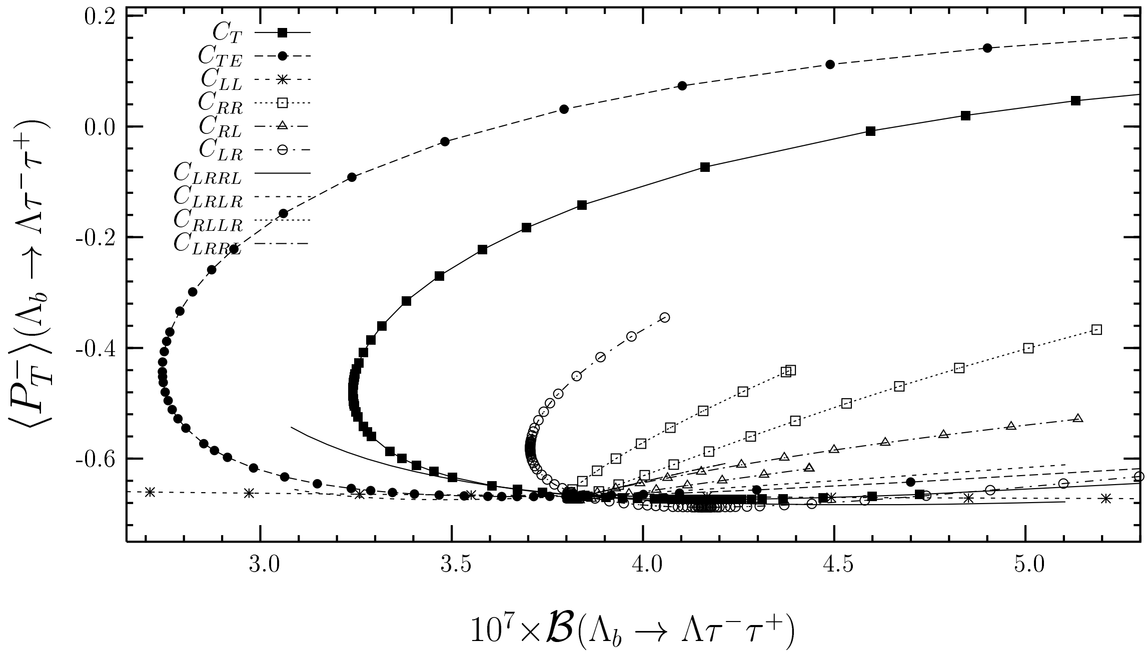

C_T
C_{TE}
C_{LL}
C_{RR}
C_{RL}
C_{LR}
C_{LRRL}
C_{LRLR}
C_{RLLR}
C_{LRRL}
$\langle P_T^- \rangle(\Lambda_b \to \Lambda \tau^- \tau^+)$
$10^7 \times \mathcal{B}(\Lambda_b \to \Lambda \tau^- \tau^+)$
0.2
0.0
-0.2
-0.4
-0.6
3.0
3.5
4.0
4.5
5.0

Fig. 6

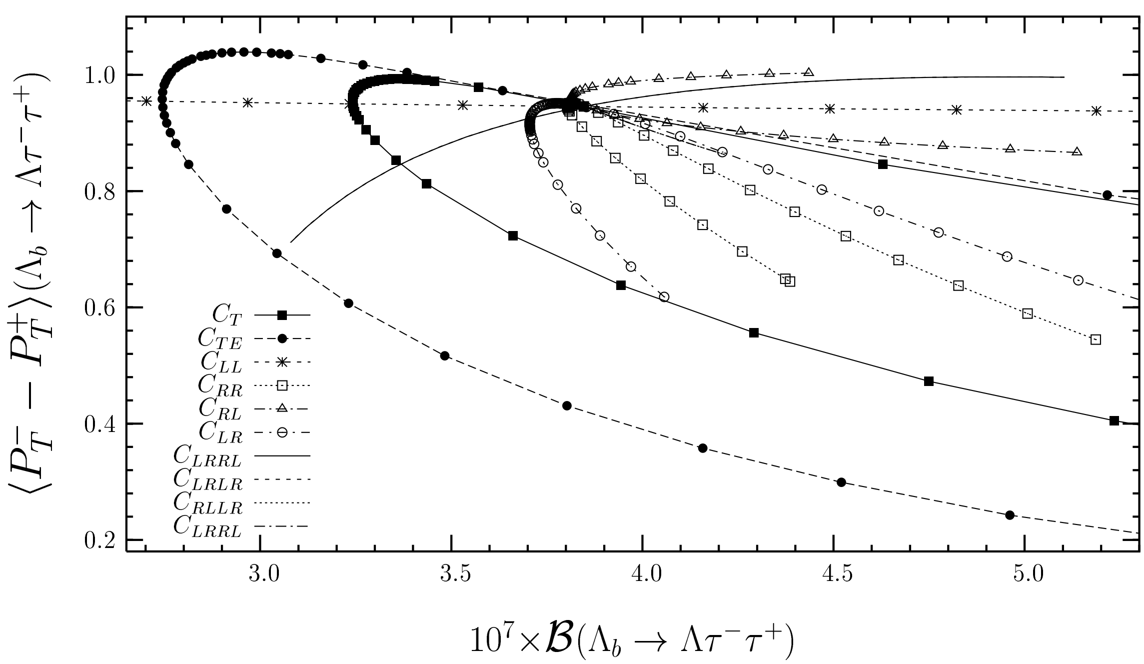

C_T
C_{TE}
C_{LL}
C_{RR}
C_{RL}
C_{LR}
C_{LRRL}
C_{LRLR}
C_{RLLR}
C_{LRRL}
$\langle P_T^- - P_T^+ \rangle(\Lambda_b \to \Lambda \tau^- \tau^+)$
$10^7 \times \mathcal{B}(\Lambda_b \to \Lambda \tau^- \tau^+)$
1.0
0.8
0.6
0.4
0.2
3.0
3.5
4.0
4.5
5.0

Fig. 7

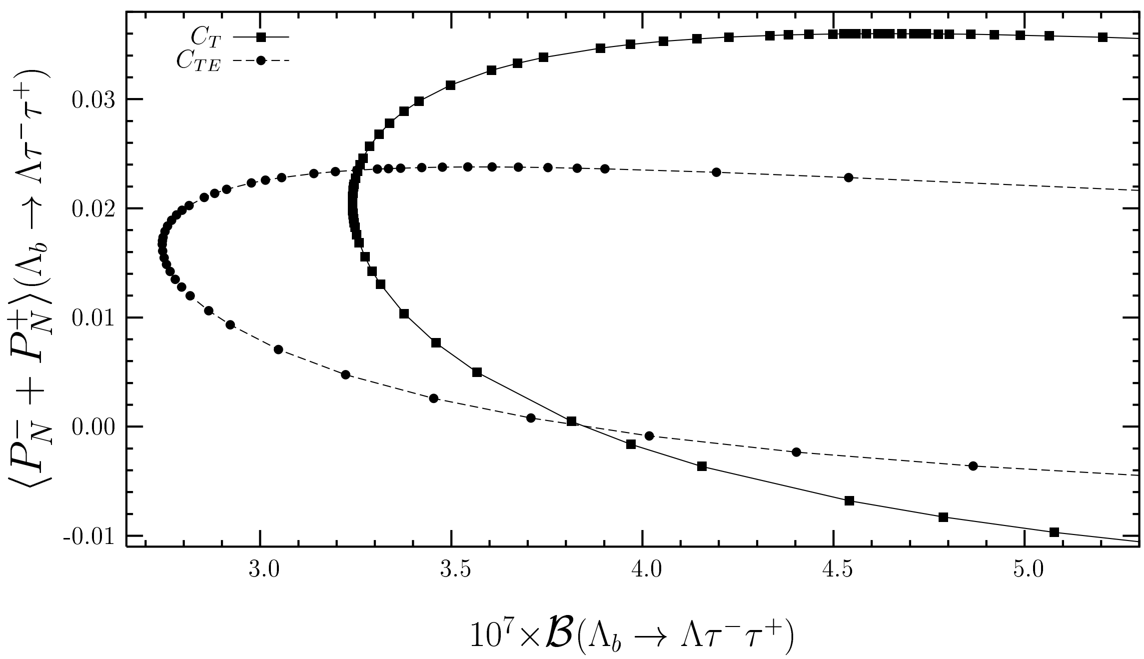
C_T
C_{TE}
0.03
0.02
0.01
0.00
-0.01
3.0
3.5
4.0
4.5
5.0
$\langle P_N^- + P_N^+ \rangle (\Lambda_b \to \Lambda \tau^- \tau^+)$
$10^7 \times \mathcal{B}(\Lambda_b \to \Lambda \tau^- \tau^+)$

Fig. 8